Aquatic Toxicology 212 (2019) 233–240

Contents lists available at ScienceDirect

Aquatic Toxicology

journal homepage: www.elsevier.com/locate/aqtox

Effects of corexit 9500A and Corexit-crude oil mixtures on transcriptomic pathways and developmental toxicity in early life stage mahi-mahi (*Coryphaena hippurus*)

Justin B. Greer[a,*], Christina Pasparakis[b], John D. Stieglitz[c], Daniel Benetti[c], Martin Grosell[b], Daniel Schlenk[a,d]

[a] Department of Environmental Sciences, University of California, Riverside, CA, United States
[b] Department of Marine Biology and Ecology, University of Miami, Miami, FL, United States
[c] Deptartment of Marine Ecosystems and Society, University of Miami, Miami, FL, United States
[d] Institute of Environmental Health, College of Environmental and Resource Sciences, Zhejiang University, Hangzhou, 310058, China

ARTICLE INFO

Keywords:
Polyaromatic hydrocarbon
Developmental toxicity
Gene expression

ABSTRACT

Crude oil and polycyclic aromatic hydrocarbon (PAH) exposure in early life stage fish has been well-characterized to induce phenotypic malformations such as altered heart development and other morphological impacts. The effects of chemical oil dispersants on toxicity are more controversial. To better understand how chemical dispersion of oil can impact toxicity in pelagic fish, embryos of mahi-mahi (*Coryphaena hippurus*) were exposed to three concentrations of the chemical dispersant Corexit 9500A, or Corexit 9500A-oil mixtures (chemically enhanced water accommodated fractions: CEWAF) of *Deepwater Horizon* crude oil for 48 h. RNA sequencing, gene ontology enrichment, and phenotypic measurements were conducted to assess toxicity. Exposure to Corexit 9500A altered expression of less than 50 genes at all concentrations (2.5, 5, and 10 mg/L nominal concentration) and did not induce acute mortality or phenotypic malformations, corroborating other studies showing minimal effects of Corexit 9500A on developing mahi-mahi embryos. CEWAF preparations contained environmentally relevant ΣPAH concentrations ranging from 1.4 to 3.1 µg/L and similarly did not alter larval morphology. Differentially expressed genes and significantly altered pathways related to cardiotoxicity, visual impairments, and Ca^{2+} homeostasis reinforced previous work that expression of genes associated with the heart and eye are highly sensitive molecular endpoints in oil-exposed early life stage fish. Differential expression and gene ontology pathways were similar across the three CEWAF treatments, indicating that increased chemical dispersion did not alter molecular outcomes within the range tested here. In addition, significant sublethal molecular responses occurred in the absence of observable phenotypic changes to the heart, indicating that effects of oil on early life stage fish may not be completely dependent on cardiac function.

1. Introduction

The *Deepwater Horizon* (*DWH*) oil spill in 2010 released millions of gallons of crude oil into the Gulf of Mexico (GoM), causing extensive oiling of the pelagic zone (Beyer et al., 2016). Following the spill, the chemical dispersants Corexit 9500A and Corexit 9527 were applied extensively at both the well-head and in surface waters in an effort to reduce slick formation and enhance oil biodegradation. An unprecedented volume of nearly 2 million gallons of Corexit were applied, and an estimated 16% of *DWH* oil was chemically dispersed. (Gray et al., 2014). Dioctyl sodium sulfosuccinate (DOSS), an anionic surfactant found in Corexit 9500A, was measured at concentrations ranging from 2 to 12 µg/L in the water column following the spill (Kujawinski et al., 2011). Furthermore, the timing of these events coincided with the spawning season for many pelagic fish species in the GoM, including mahi-mahi (*Coryphaena hippurus*, referred to as mahi in the following). It is therefore likely that early life stage (ELS) fish, which are particularly vulnerable to environmental pollutants, were exposed to dispersants as well as crude oil and its derivatives (Rooker et al., 2013).

Crude oil toxicity is correlated with the concentration of solubilized 3-ring PAHs and varies greatly depending on oil source, state of weathering, UV exposure, and other factors. *DWH* oil collected from both the well-head and surface impairs cardiac development and

* Corresponding author at: Department of Environmental Sciences, University of California Riverside, 2460A Geology, Riverside, CA, 92521, United States.
E-mail address: jgreer@ucr.edu (J.B. Greer).

https://doi.org/10.1016/j.aquatox.2019.05.014
Received 10 March 2019; Received in revised form 20 May 2019; Accepted 21 May 2019
Available online 23 May 2019
0166-445X/

function in ELS fish. Environmentally relevant concentrations of crude oil were found to induce pericardial edema, reduce cardiomyocyte function, and alter cardiac development in several GoM species (Brette et al., 2014; Incardona et al., 2014; Khursigara et al., 2017; Pasparakis et al., 2016). In mahi, reduced cardiac performance has been linked with altered swim performance in juveniles that could affect survival in the wild (Mager et al., 2014). While many cardiotoxic effects of oil occur via activation of aryl-hydrocarbon receptors (AhR) and altered mitochondrial function (Lanham et al., 2014), oil also induces many non-AhR-mediated changes that could contribute to cardiotoxicity and other developmental abnormalities; including alterations in craniofacial development, eye size, and yolk sack edema (Incardona, 2017).

The acute toxicity of Corexit 9500A exposure in ELS fish native to the Gulf of Mexico has been extensively studied. Corexit 9500A 10% effect concentrations (LC_{10}) in ELS pelagic (mahi, Florida pompano, *Trachinotus carolinus*; Atlanta bluefin tuna, *Thunnus thynnus*) and estuarian (*Cyprinodon variegatus*) fish generally exceed 10 mg/L, far above Corexit concentrations measured after the spill, and suggest that significant acute effects of Corexit alone were unlikely to occur at environmentally relevant concentrations (Dasgupta et al., 2015; Echols et al., 2018; Edmunds et al., 2015; Esbaugh et al., 2016; National Academies of Sciences and Medicine, 2019). However, none of the aforementioned studies examined the potential for molecular alterations and other sublethal effects that did not result in acute lethality in ELS fish. In adult fish Jones et al. (2017) observed that exposure of the nearshore species *Cyprinodon variegatus* to 1000 ppm Corexit 9500A induced more differentially expressed genes in liver than crude oil, with genes involved in immune function significantly affected.

The effects of chemical dispersion on oil toxicity are also variable. In many species, increased mortality, developmental deformities, reduced growth, and increased induction of stress response genes have been reported in chemically dispersed oil compared to oil alone (Mu et al., 2014; Ramachandran et al., 2004). However, the addition of Corexit 9500 did not alter acute mortality or cardiotoxicity of oil preparations in mahi embryos (Esbaugh et al., 2016). Other studies have also found little to no effects of dispersants on oil toxicity (Fuller et al., 2004; Hemmer et al., 2011).

The aim of this study was to assess the transcriptomic and phenotypic effects of Corexit 9500A and Corexit 9500A-oil mixtures on mahi embryos. The current study is the first to assess the transcriptomic impacts of Corexit 9500A and oil-dispersant mixtures on embryos of a pelagic species in the GoM, and to determine if molecular responses can occur prior to phenotypic changes in cardiac function in ELS fish following oil exposure.

2. Methods

2.1. Oil preparation

Mahi embryos were exposed to chemically-enhanced water-accommodated fractions (CEWAFs) or Corexit 9500A alone. CEWAFs were prepared with oil from the surface collected during the *DWH* oil spill (referred to herein as OFS). Oil samples were collected via skimming operations from surface waters by British Petroleum for testing purposes, and subsequently transferred under chain of custody to the University of Miami (sample ID: OFS-20100719-Juniper-001 A0087 M). Three CEWAFs were prepared in 1-L glass jars at a nominal loading of 1 g of oil per liter of 1 µm filtered, UV-sterilized seawater. Corexit 9500A was then added at a rate of 50, 100, or 200 mg g of oil. The mixtures were stirred overnight in darkness for approximately 18–24 hours and left to settle for 3–6 hours before use. The lower 90% of the mixture was then carefully drained and retained for subsequent use as 100% CEWAF (unfiltered). CEWAFs were diluted to 5% using UV-sterilized seawater for test exposures, for final Corexit 9500A nominal concentrations of 2.5, 5, or 10 mg/L (referred to as CEWAF low, medium, and high throughout). The highest nominal concentration of Corexit 9500A (10 mg/L) was based on LC20 concentrations for Corexit 9500 in mahi from a previous study (Esbaugh et al., 2016).

Corexit 9500A only exposures were prepared in a 1-L glass jar at a nominal loading of 200 mg per 1-L of seawater. The mixture was stirred overnight, allowed to settle, and drained similarly to the CEWAF preparations. The undiluted Corexit 9500A was then diluted to obtain three final nominal concentrations; 2.5, 5, and 10 mg/L (referred to as Corexit 9500A low, medium, and high throughout).

2.2. Experimental design

Mahi embryos were obtained from a natural volitional spawning event of captive wild mahi broodstock caught off the coast in Miami, FL. Fish were maintained at the University of Miami Experimental Hatchery (UMEH) as detailed in Stieglitz et al. (2017). Mahi broodstock at the UMEH produce embryos and larvae of high and constant quality (Kloeblen et al., 2018). The embryos were subsequently transferred from UMEH to the embryo exposure laboratory at Rosenstiel School of Marine and Atmospheric Science (RSMAS) around 8 h post fertilization (hpf) and immediately transferred into 1 L glass beakers (30 embryos per beaker). The mahi embryos were exposed to sublethal doses of Corexit 9500A or CEWAF treatments as described above for 48 h. Seawater controls were performed concurrently with exposures using the same 1 µm filtered UV-sterilized seawater used in exposure preparation. After 48 h, larvae were sampled and frozen in liquid nitrogen for subsequent transcriptomic analysis or imaged for phenotypic endpoints. The phenotypic and transcriptomics experiments were performed independently on different dates and using different batches of embryos. Exposures were conducted in a temperature and light controlled-room (photoperiod: 12L: 12D; temperature: 25 °C). Aeration was not used in order to reduce PAH depletion over the 48 h exposure period.

2.3. Water chemistry analysis

Water chemistry samples were collected before and after the exposure period and are reported as geometric means to account for PAH depletion over the 48 h of exposure for the morphological experiments. For the RNASeq study samples were collected prior to exposure only. Oil samples were collected in 250 mL amber glass bottles with no head space and immediately stored at 4 °C. Sample bottles were shipped overnight on ice to ALS Environmental (Kelso, WA) for analysis by gas chromatography/mass spectrometry- selective ion monitoring (GC/MS-SIM; based on EPA method 8270D). Reported ΣPAH values represent the sum of 50 PAH analytes, selected by the EPA based on individual toxicity and concentration in water.

CEWAF and Corexit 9500A samples were collected at the start of the exposure period and stored in four 10 ml falcon tubes at 4 °C. Samples were shipped overnight to ALS Environmental (Kelso, WA) for DOSS analysis. To monitor ambient holding conditions, the following water quality parameters were measured at approximately that same time each day (12:00 − 13:00): temperature, pH, dissolved oxygen (DO), salinity, and total ammonia. Temperature and DO were measured using a ProODO hand held optical DO probe and meter (YSI, Inc., Yellow Springs, OH) and pH was measured using a pH meter (Hach, Loveland, CO) fitted with a combination glass electrode. The pH and DO probes were calibrated daily. Salinity was measured using a refractometer and total ammonia determined using a micro- modified colorimetric assay (Ivančič and Degobbis, 1984). Water quality parameters are presented in **Tables S1 and S2**.

2.4. Phenotypic measurements

Prior to imaging, the number of surviving mahi larvae were counted for mortality assessment in each 1 L beaker. Ten larvae were then

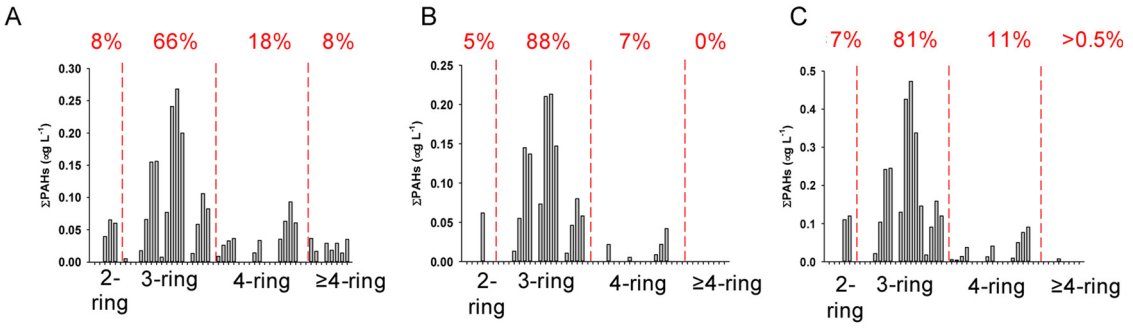

D

CEWAF nominal Corexit 9500A conc. (mg/L)	DOSS conc. (µg/L)	∑50PAH (µg/L)	∑3-ring PAHs (µg/L)
2.5	210	2.20	1.45
5	380	1.35	1.19
10	650	3.09	2.51

Fig. 1. PAH composition of CEWAF preparations prior to RNASeq. Nominal DOSS concentrations of 2.5 mg/L (A), 5.0 mg/L (B), and 10 mg/L (C). (D) Measured concentrations of DOSS, Σ50PAH, and Σ3-ring PAHs in CEWAF preparations for RNASeq.

randomly chosen from each treatment, placed in 2% methyl cellulose in seawater, and immediately mounted and imaged on a Nikon SMZ800 stereomicroscope. Images were taken of each larvae using iMovie software and later assessed for pericardial area, yolk sac area, and eye diameter using ImageJ version 1.52a (Schneider et al., 2012). Heart rate was determined by counting the number of heart beats in 15 s video clips.

2.5. RNA purification, library preparation, and sequencing

After 48 h treatment exposures surviving larvae were collected from three biological replicates per treatment, each biological replicate containing 15–30 surviving larvae. Frozen larvae were lysed in Buffer RLT (Qiagen), homogenized using a Kontes Pellet Pestle Cordless Motor (Sigma-Aldrich, St. Louis, Missouri), and total RNA extracted using the RNeasy mini kit (Qiagen). Total RNA concentration was quantified using a Qubit Fluorometer and RNA quality and integrity assessed using an Agilent 2100 Bioanalyzer. Only high-quality RNA samples with a RIN score > 7 on the Bioanalyzer were used for downstream library preparation.

mRNA was isolated from 500 ng of total RNA using the NEBNext Poly(A) mRNA Magnetic Isolation Module, and the resulting mRNA prepared using the NEBNext Ultra II Directional RNA Library Prep Kit (New England Biolabs, Ipswich, Massachusetts). Final complementary DNA libraries were assessed on an Agilent 2100 Bioanalyzer (Agilent Technologies, Palo Alto, CA) to verify proper fragment sizes, and library concentrations were quantified using the Qubit Fluorometer. Libraries were multiplexed and sequenced as single-end 75 bp reads by the University of California Riverside genomics facility (Riverside, CA) in one lane of a NextSeq500 high-throughput sequencer (Illumina). Raw sequencing reads were submitted to the NCBI SRA database (Accession: PRJNA512294).

2.6. Bioinformatic analysis

Prior to downstream analysis, read quality was assessed using FastQC (version 0.11.7) (Andrews, 2010). Adapter trimming and removal of poor quality reads were performed using trimmomatic (version 0.36) (Bolger et al., 2014) with the following parameters: ILLUMINACLIP:TruSeq3-SE.fa:2:30:10 LEADING:5 TRAILING:5 SLIDINGWINDOW:4:15 MINLEN:25. After trimming, read quality was again assessed with FastQC. Trimmed reads were pooled and used to assemble a *de novo* transcriptome with Trinity (version 2.6.6) (Haas et al., 2013) with strand specific read orientation and in silico read normalization. All other parameters were kept as the defaults. Transcript abundance was assessed by aligning trimmed reads back to the Trinity assembly with bowtie2 (version 2.3.4.1) (Langmead and Salzberg, 2012) and quantification with RSEM (version 1.3.0) (Li and Dewey, 2011). Abundance estimates for each gene are calculated in RSEM by generating Maximum Likelihood abundance estimates using the Expectation-Maximization algorithm as described in Li and Dewey (2011). Quantification was used to assess differential expression in DESeq2 (version 1.20.0) (Love et al., 2014) at $p \leq 0.05$ after Benjamini-Hochberg false discovery rate correction (Benjamini and Hochberg, 1995).

Functional annotation of Trinity transcripts was performed using the Trinotate package (version 3.1.1), with transcripts annotated using BLASTp, Swissprot (Bairoch et al., 2004), and Pfam (Finn et al., 2013). Transcripts that were differentially expressed and annotated, and their log-fold changes, were input into Ingenuity Pathway Analysis (IPA) and the Database for Annotation, Visualization and Integrated Discover (DAVID) to identify molecular and biological pathways that may have been altered at a significance of $p \leq 0.05$ after Benjamini-Hochberg false discovery rate correction.

3. Results

3.1. Chemical composition of Corexit and CEWAF preparations

Measurements of DOSS, a commonly measured surfactant in Corexit 9500A, were used to estimate Corexit 9500A concentrations. Previous studies have estimated that DOSS comprises ~15% of the total Corexit 9500A composition (Jones et al., 2017). Measured DOSS concentrations in Corexit 9500A treatments were 420 µg/L in the low exposure (nominal concentration 2.5 mg/L), 620 µg/L in the medium exposure (nominal concentration 5 mg/L), and 1100 µg/L in the high exposure (nominal concentration 10 mg/L). Thus, DOSS comprised 11–16.8% of Corexit 9500A by weight.

Measured Σ50PAH concentrations in 5% CEWAF preparations for RNASeq were 2.2, 1.4, and 3.1 µg/L in the low, medium, and high Corexit 9500A concentrations, respectively (Fig. 1D**, Table S3 for all PAHs**). The medium Corexit concentration contained the lowest total

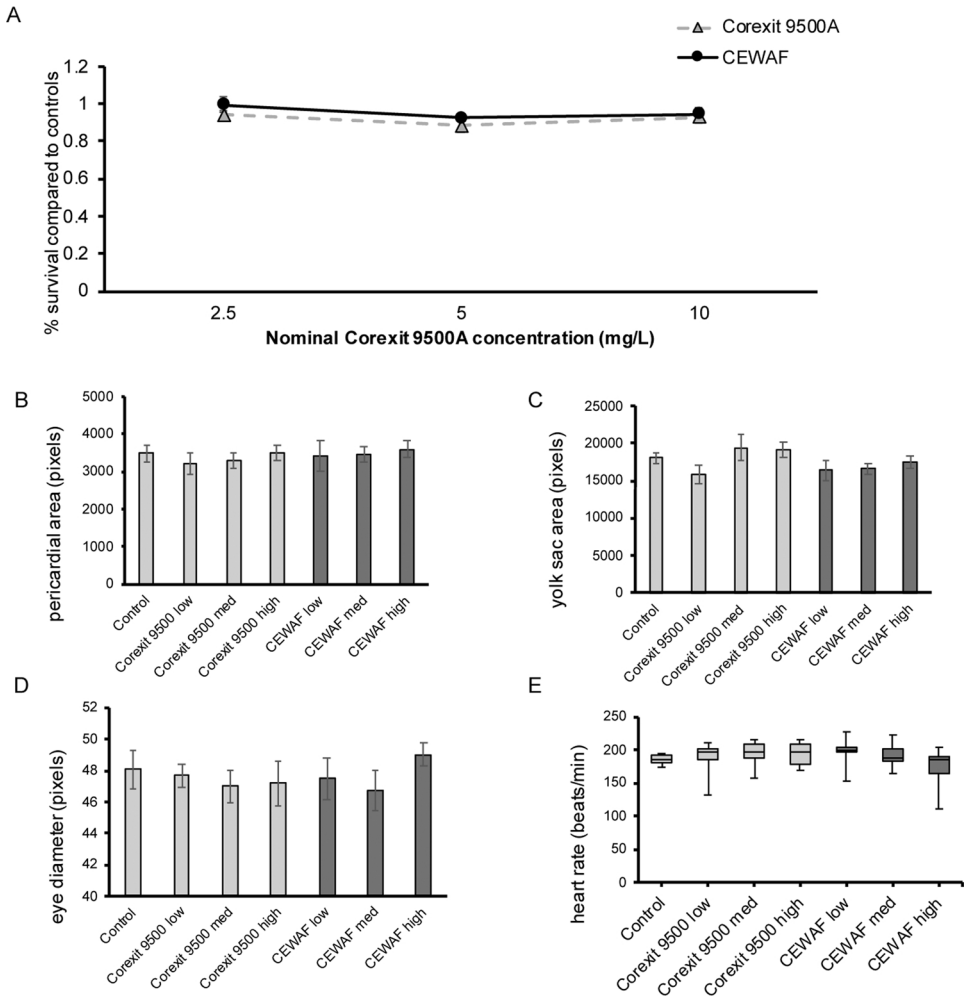

Fig. 2. Phenotypic measurements for Corexit 9500A and CEWAF exposures. (A) Number observed alive 48 h after exposure, compared to proportion alive in the control group (n = 8). Measurements of pericardial area (B), yolk sac area (C), eye diameter (D), and heart rate (E) in mahi larvae 48 hpf (n = 10). All data are presented as mean ± SEM. There were no significant differences in mortality or phenotypic changes in any treatments (one-way ANOVA, $p \leq 0.05$).

PAHs and contained the fewest amount of highly toxic 3-ring PAHs (Fig. 1D). CEWAF preparations for phenotypic analysis contained similarly low ΣPAH concentrations (geometric mean 0.7–1.0 µg/L; **Table S4**), with DOSS concentrations of 290, 550, and 890 µg/L.

3.2. Mortality and phenotypic measurements

During the phenotype study mean survival in the controls was 92.9% ± 1.8% (mean ± SEM), and none of the Corexit 9500A or CEWAF treatments resulted in a significant difference in mortality compared to controls (Fig. 2A). In the RNASeq study survival was significantly reduced only in the low Corexit 9500A concentration, suggesting that this effect was not dispersant-related (**Fig S2**, mean control survival 85% ± 1.6%). There were no significant differences in pericardial area, yolk sac area, or eye diameter observed with any treatments (Fig. 2**B-D**). There were also no significant differences observed for heart rate in any treatments. However, there was a trend towards decreased heart rate in the highest CEWAF treatment (Fig. 2E).

3.3. Transcriptome assembly statistics and sample correlations

Greater than 99% of the raw reads passed quality filtering, resulting in ˜540 million reads (˜25.5 million reads/replicate) for use in downstream transcriptome assembly (Table S**5**). Strand specificity of library preparation was confirmed using the examine_strand_specificity.pl script in Trinity (Fig S**3**). *De novo* transcriptome with Trinity assembled a total of 224,003 genes with an N50 contig length of 1021 bp based on the longest isoform per gene, and > 90% of the reads aligned back to transcriptome using bowtie2, indicating that transcriptome assembly was representative of the reads. Transcriptome annotation via Trinotate identified 15,810 uniquely annotated genes from the Trinity assembly.

The relationship between samples was calculated using a sample correlation heatmap (Fig. 3A**)** and principle component analysis (PCA). Hierarchical clustering in the heatmap dendrogram shows all CEWAF treatments cluster together, with a separate clade containing Corexit 9500A and negative controls. This shows that the addition of oil, despite low Σ50PAH concentrations, altered the overall transcriptomic profile in mahi embryos. Within each clade there were no obvious correlations between Corexit 9500A concentration and the transcriptome. The lone exception was the high Corexit 9500A treatment, which had highly variable gene expression across the three biological replicates. The PCA corroborated the sample correlation heatmap results, with clear differences between CEWAF and Corexit 9500A treatments, but little effect of varying Corexit 9500A concentrations (Fig. 3B).

3.4. Differentially expressed genes

Compared to controls there were 14, 41, and 8 differentially expressed genes in low, medium, and high Corexit 9500A treatments,

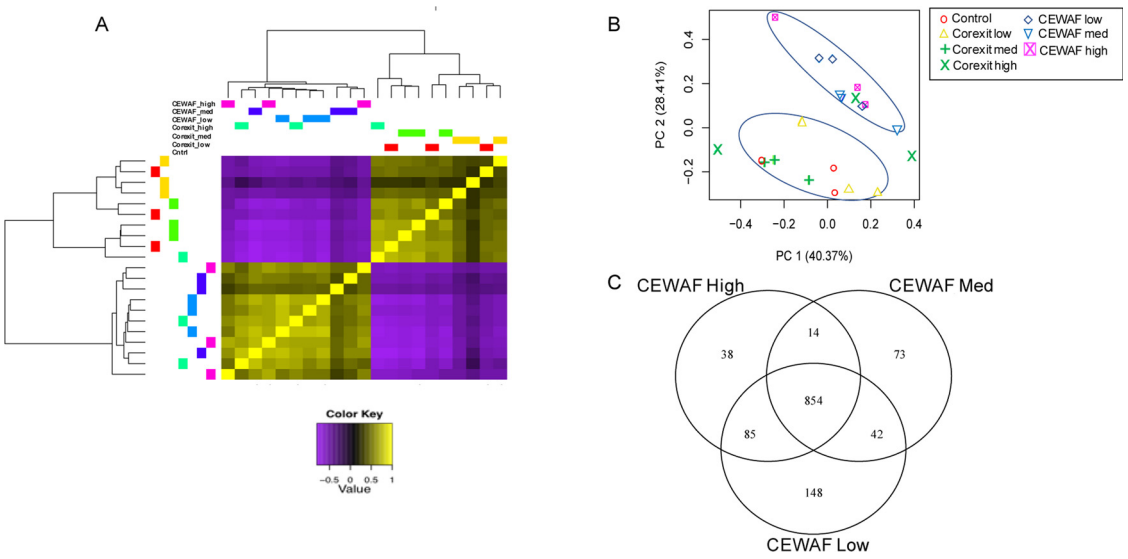

Fig. 3. (A) Heatmap dendrogram of sample correlations. (B) Principle component analysis of transcriptomic profiles. Circles represent separate clusters formed by CEWAF exposures and control + dispersant treatments. The highest Corexit 9500A concentration (green x) was highly variable across biological replicates. (C) Venn diagram of overlapping differentially expressed genes ($p \leq 0.05$) across CEWAF treatments.

respectively. There were also fewer than 50 differentially expressed genes when comparing across Corexit 9500A treatments.

There were 1129, 983, and 991 annotated differentially expressed genes in respective CEWAF low, medium, and high treatments compared to controls. Furthermore, there was a high degree of overlap in the genes that were differentially expressed across the CEWAF treatments (Fig. 3C). Cytochrome P450 1A1 (*cyp1a1*), a prominent gene upregulated during PAH exposure, had the highest log fold change in all three CEWAF treatments (Fig. 4A), and cytochrome P450 1B1 (*cyp1b1*) was also in the top three most upregulated genes. Neither of the aforementioned cytochrome p450's were differentially expressed in Corexit treatments. Many mitochondrial genes were found to be differentially expressed in CEWAF treatments, including cytochrome c oxidase, ATP synthase F(0) complex, mitochondrial heat shock proteins 10 kDa and 60 kDa, and several subunits of NADH dehydrogenase.

3.5. Pathway analysis

Canonical pathways, biological functions, and toxicity outcomes predicted to be altered by exposure were assessed using the IPA pathway analysis tool. Biological processes, molecular functions, and cellular components predicted to be affected were also assessed using DAVID to supplement IPA results. Due to the low numbers of differentially expressed genes in Corexit 9500A treatments, pathway analyses were performed only on CEWAF exposures. Out of the 15,810 unique genes identified during transcriptome assembly 9862 (62%) were mapped in IPA and used for downstream pathways analysis.

Because of the high degree of overlap of differentially expressed genes, many of the pathways altered were consistent between CEWAF treatments. IPA predicted mitochondrial dysfunction as the most significantly altered canonical pathway in all three CEWAF treatments. Similarly, in DAVID ATP hydrolysis was the top biological process and mitochondrial inner membrane was one of the top cellular components predicted to be altered. Oxidative phosphorylation and calcium

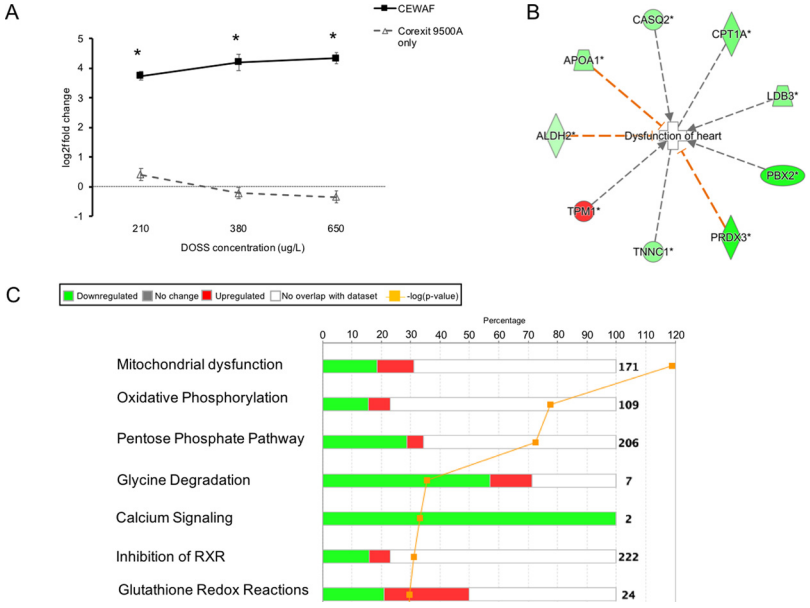

Fig. 4. (A) Cyp1a1 expression compared to controls in CEWAF and Corexit 9500A treatments. Values expressed as mean ± SE. * represents $p \leq 0.05$ after FDR correction. (B) Down-regulation of cardiac genes in CEWAF high exposure that are predicted by IPA to induce heart dysfunction. (C) Top canonical pathways altered by CEWAF treatments.

signaling were also in the top 5 most significantly altered canonical pathways in all three CEWAF treatments with IPA (Fig. 4C). Stress response pathways were also highly represented in IPA, with NRF2-mediated oxidative stress response, aryl hydrocarbon receptor signaling, and production of nitric oxide and reactive oxygen species were also indicated. Endoplasmic reticulum stress pathway was listed in the top 25 pathways for only the medium CEWAF treatment.

Many of the top diseases and biological functions predicted in IPA to be activated are associated with cell death and survival, including necrosis and apoptosis (**Table S6**). In contrast, functions predicted to be diminished after exposure were primarily involved in general cellular metabolism such as protein synthesis, fatty acid metabolism, efflux of cholesterol, and synthesis of lipids. Several other pertinent diseases and biological functions without predicted activation or deactivation were involved in neurological abnormalities including neuromuscular disease, and movement disorders. **Table S6** contains the top 20 significantly enriched functions from IPA for each CEWAF treatment. DAVID does not provide disease or toxicity function categories for comparison to IPA results.

Although the order of significance differed between CEWAF treatments, toxicity functions in IPA overwhelmingly targeted cardiac and hepatic functions (**Table S7**). Eight of the top 10 toxicity functions from IPA were associated with cardiac malformations in the highest CEWAF treatment: including 18 genes associated with cardiac dilation and cardiomyopathy. Only a few organ-based pathways were identified in DAVID. Cardiac muscle contraction through impacts on the regulation of sequestered Ca^{2+} release was a significantly affected biological process, and impacts on visual perception were also predicted to be affected (biological processes #15) in DAVID, which was not observed in IPA.

4. Discussion

Assessment of oil toxicity following major oil spills is difficult due to complex interactions between oil source, weathering, and chemical dispersion. Furthermore, lowest observable effect concentrations (LOEC) for cardiotoxic endpoints such as pericardial edema are species and oil specific and can range from less than 1 μg/L ΣPAH to greater than 30 μg/L, further complicating damage assessments (Incardona et al., 2014, 2013; Khursigara et al., 2017; Perrichon et al., 2018). To better understand the morphological and molecular impacts of dispersed oil on early life stages of fish, we evaluated the transcriptomic and phenotypic developmental impacts of the chemical dispersant Corexit 9500A, and chemically dispersed *DWH* surface oil on a pelagic species native to the GoM.

Addition of chemical dispersants Corexit 9500A and Corexit 9527 following the *DWH* oil spill enhanced the dissolution of water soluble components of the oil with the purpose of reducing volatile hydrocarbon exposures to direst responders, enhancing biodegradation and mitigating impact of surface slicks on wildlife and shoreline habitats (National Academies of Sciences and Medicine, 2019). This process increased availability of 3-ring PAHs (Couillard et al., 2005), such an phenanthrene, which have been shown to be a source of physiological disruptions leading to cardiac dysfunction (Brette et al., 2017; Esbaugh et al., 2018; Incardona et al., 2004). However, we did not observe a relationship between increasing Corexit 9500A concentration and an enhanced fraction of dissolved PAHs. Generally, chemical dispersants are applied to recent oil spills that are less weathered and have a higher potential for dispersal than the highly weathered slick oil used in this study. This was also evident in our gross observations of poor oil dispersion of the CEWAF preparations following overnight mixing. These factors may explain the consistently low ΣPAH concentrations observed at all Corexit 9500A loading concentrations and limits our ability to assess the relationship between Corexit concentration and the fraction of dissolved PAHs in this study. We also did notobserve a relationship between increasing Corexit 9500A concentration and mortality, incidences of phenotypic malformations, or increased differential gene expression. This parallels other studies in mahi and other marine fish showing that acute mortality is directly correlated with the fraction of soluble PAHs and not dispersant to total oil exposure (Adams et al., 2014; Esbaugh et al., 2016; Mu et al., 2014). Σ50PAH concentrations obtained in this study ranged from 0.8 to 3.1 μg/L, which are below LC_{50} concentrations (9.5 μg/L), the LOEC for reduced atrial contractility (3.5 μg/L), and EC_{50} concentrations for pericardial edema (13.0 μg/L) in mahi exposed to slick oil CEWAFs (Esbaugh et al., 2016).

Molecular and phenotypic endpoints indicated that Corexit 9500A had little impact on mahi larvae. Relatively few genes were differentially expressed, and Corexit 9500A and negative control treatments clustered together in sample correlations. This is consistent with many other studies showing limited acute Corexit-induced toxicity in ELS fish native to the Gulf of Mexico (Dasgupta et al., 2015; DeLorenzo et al., 2018; Echols et al., 2018; Edmunds et al., 2015; Esbaugh et al., 2016), and supports predictions that Corexit 9500A toxicity does not occur until the critical micellar concentration of 1.25 mg/L in seawater (Steffy et al., 2011). Furthermore, DOSS concentrations in this study (420–1100 μg/L) were well above DOSS concentrations measured in the GoM in the months following the spill (2–12 μg/L), and Corexit is rapidly biodegraded at water temperatures experienced in the Gulf of Mexico during the summer months (Campo et al., 2013), together suggesting that ecologically relevant concentrations of dispersants may have had little direct impact on ELS pelagic fish in the GoM. In contrast, other studies have reported that Corexit may decrease sperm fertilizing ability in teleost fish at 500 μL/ 1 L (Beirão et al., 2018) and elicits a substantial molecular response in the liver of adult sheepshead minnow (Jones et al., 2017). These findings indicate that life stage and tissue may play an important role in dispersant toxicity.

While Corexit 9500A failed to significantly alter gene expression in mahi embryos, CEWAF exposures caused changes in ion signaling consistent with earlier studies in oil-treated mahi. Dysregulation of tightly coordinated Ca^{2+} fluxes in cardiomyocytes has been proposed to contribute to cardiac arrhythmia, disruptions in excitation-contraction coupling, and reduced cardiomyocyte function in oil-exposed larvae (Brette et al., 2014, 2017). Previous transcriptomic studies have consistently observed alterations in cardiac genes important for Ca^{2+} cycling and Ca^{2+} signaling that may contribute to physiological disruptions (Sørhus et al., 2017; Xu et al., 2017, 2016). Consistent with those studies, we also observed downregulation of several cardiac Ca^{2+} homeostasis genes and enrichment of cardiotoxic pathways, even in the absence of phenotypic differences. Cardiac muscle troponin *(tnnt2)* and calsequestrin 2 (*casq2*) regulate intracellular Ca^{2+} and are essential for proper function of cardiomyocyte sarcomeres (Knollmann et al., 2006; Sehnert et al., 2002). *Casq2* was downregulated in all CEWAF exposures and *tnnt2* was downregulated in the highest concentration (ΣPAH 3.09 μg/L). Both *tnnt2* and *casq2* were also differentially expressed in a previous transcriptomic study in mahi using slick oil with higher ΣPAH concentrations (Xu et al., 2016). Furthermore, morpholino knockdown of *tnnt2* in zebrafish (*Danio rerio*) embryos induces cardiac defects nearly identical to 3-ring PAHs (Incardona et al., 2004; Sehnert et al., 2002). Together this suggests that *tnnt2*- and *casq2*-induced Ca^{2+} dysregulation may be intimately involved in Ca^{2+} cycling disruptions in the sarcoplasmic reticulum, leading to disruptions in excitation-contraction coupling in oil-exposed fish. Other Ca^{2+} homeostasis genes altered were unique to this study. Troponin C (*tnnc1*) binds Ca^{2+} and is essential for activation of cardiac muscle contractions (Duan et al., 2016; Li and Hwang, 2015) and was downregulated in all 3 CEWAF exposures. LIM domain binding protein (*ldb3*) was also downregulated, which stabilizes sarcomeres during cardiac contractions (Pashmforoush et al., 2001). Taken together with previous studies (Brette et al., 2014; Xu et al., 2017, 2016), these data provide strong molecular evidence that Ca^{2+} perturbations are an important component of PAH-induced toxicity.

Phenotypic malformations in larval fish may not manifest until later

life stages, well after the molecular initiating events of the first several days (Sørhus et al., 2017), and could explain the observation of molecular alterations in the absence of phenotypic differences in cardiac performance. Using a less weather *DWH* slick oil, PAH concentrations of 1.2 µg/L reduced swimming performance in mahi embryos-larvae nearly a month after exposure (Mager et al., 2014). However, molecular endpoints were not measured during this previous study, and thus it is unclear if molecular alterations similar to those observed here were the initiating events for latent declines in swim performance. Further studies over a longer time course would be needed to determine if ELS molecular changes, such as those observed here, are diagnostic of health impairments at later life stages.

It has also been suggested that non-cardiac effects of PAH exposure are secondary effects of reduced cardiac output (Incardona et al., 2004). However, in this study we observed that neurological pathways were prominently altered at low PAH concentrations and in the absence of cardiac defects. Significant molecular effects on neurological pathways have also been observed in mahi at higher PAH concentrations (15 µg/L) (Xu et al., 2016). Furthermore, behavioral declines in habitat settlement and antipredator behaviors occur in reef fish at PAH concentrations ≤5.7 µg/L, indicating that higher-order cognitive processes may be directly impaired by PAHs (Johansen et al., 2017). There was also significant enrichment of the visual perception pathway predicted by DAVID in CEWAF exposed larvae compared to controls. This is consistent with previous studies reporting that optomotor and visual responses are affected in mahi and red drum larvae at PAH concentrations as low as 0.67 and 2.72 µg/L, respectively. This suggests that visual impairment is an equally or possibly more sensitive endpoint than cardiotoxicity in these fish (Magnuson et al., 2018; Xu et al., 2018). Specific genes altered included retinol dehydrogenase 12 (*rdh12*), a key enzyme in 11-cis-retinal formation during regeneration of visual pigments in cones, and phosducin, which may regulate photoreceptor function (Haeseleer et al., 2002; Lee and Lolley, 1993). Previous studies using IPA indicated vision as being targeted in oil-exposed mahi, which was not observed here, likely due to low PAH concentrations. Regardless, together these data indicate that PAHs may directly target organ systems outside the heart and downstream effects may not be solely dependent on cardiac function.

Decreased total cholesterol (ΣPAH 8.3 µg/L) and changes in cholesterol biosynthesis pathways (ΣPAH 15 µg/L), possibly due to poor yolk absorption, were prominent responses in mahi at higher PAH concentrations (McGruer et al., 2019; Xu et al., 2017, 2016). At the PAH concentrations utilized in this study, cholesterol was not in the top 20 altered pathways (IPA #42). This is in agreement with other studies in which slick oil (initial Σ50PAH 3.1 µg/L) did not enrich cholesterol pathways in mahi (Xu et al., 2018). However, cholesterol was altered at higher PAH concentrations in haddock (7.6 ug/L) and red drum (4.7 µg/L) (Sørhus et al., 2017; Xu et al., 2017). Our data suggest that chemical dispersion may not enhance cholesterol impairment at the low PAH concentrations used in this study.

Unsurprisingly, AhR pathways were induced in CEWAFs, as measured by a 4-fold higher expression of *cyp1a1*. The AhR pathway regulates detoxification of PAHs via activation of xenobiotic metabolism and stress-response pathways and is consistently upregulated following oil exposure in many species (Garcia et al., 2012; Pilcher et al., 2014; Whitehead et al., 2012; Xu et al., 2017, 2016). Activation of AhR during prolonged oil exposure has been linked to impaired development and decreased survival in embryos and larvae (Whitehead et al., 2011, 2010). Taken together our RNASeq results suggest similar pathways and molecular responses as previous studies using low PAH concentrations, but without overt toxicity.

In summary, early life stage mahi exposed to the chemical dispersant Corexit 9500A were mostly unaffected, indicating that exposure to environmentally relevant concentrations of this dispersant alone is unlikely to have significant implications for ELS mahi survival. In contrast, exposure to chemically dispersed oil at environmentally relevant PAH concentrations induced significant molecular, but not phenotypic effects at 48 hp. Simultaneous molecular responses observed in ELS mahi suggest adverse effects caused by oil exposure may not solely be due to downstream effects of cardiac impairment, and increasing concentrations of Corexit 9500A had little effect on oil-induced toxicity. Pathways and genes important for cardiac function and vision were the most affected, similar to studies using slick oil without chemical dispersion, and support cardiac and visual alterations as the most sensitive endpoints of oil-induced toxicity in mahi.

Funding

This research was made possible by a grant from The Gulf of Mexico Research Initiative. Grant No. SA-1520; Name: Relationship of Effects of Cardiac Outcomes in fish for Validation of Ecological Risk (RECOVER). Data are publicly available through the Gulf of Mexico Research Initiative Information & Data Cooperative (GRIIDC) at https://data.gulfresearchinitiative.org (doi:https://doi.org/10.7266/n7-sfa3-9041).

Competing interests

The authors declare that they have no competing interests.

Acknowledgements

The authors would like to thank Dr. David Volz and Dr. Subham Dasgupta for their assistance with gene ontology analysis. MG holds a Maytag Research Chair of Ichthyology.

Appendix A. Supplementary data

Supplementary material related to this article can be found, in the online version, at doi:https://doi.org/10.1016/j.aquatox.2019.05.014.

References

Adams, J., Sweezey, M., Hodson, P.V., 2014. Oil and oil dispersant do not cause synergistic toxicity to fish embryos. Environ. Toxicol. Chem. 33, 107–114.
Andrews, S., 2010. FastQC: A Quality Control Tool for High Throughput Sequence Data.
Bairoch, A., Boeckmann, B., Ferro, S., Gasteiger, E., 2004. Swiss-Prot: juggling between evolution and stability. Brief. Bioinformatics 5, 39–55.
Beirão, J., Litt, M.A., Purchase, C.F., 2018. Chemically-dispersed crude oil and dispersant affects sperm fertilizing ability, but not sperm swimming behaviour in capelin (Mallotus villosus). Environ. Pollut. 241, 521–528.
Benjamini, Y., Hochberg, Y., 1995. Controlling the false discovery rate: a practical and powerful approach to multiple testing. J. R. Stat. Soc. Ser. B 57, 289–300.
Beyer, J., Trannum, H.C., Bakke, T., Hodson, P.V., Collier, T.K., 2016. Environmental effects of the Deepwater Horizon oil spill: a review. Mar. Pollut. Bull. 110, 28–51.
Bolger, A.M., Lohse, M., Usadel, B., 2014. Trimmomatic: a flexible trimmer for Illumina sequence data. Bioinformatics 30, 2114–2120.
Brette, F., Machado, B., Cros, C., Incardona, J.P., Scholz, N.L., Block, B.A., 2014. Crude oil impairs cardiac excitation-contraction coupling in fish. Science 343, 772–776.
Brette, F., Shiels, H.A., Galli, G.L., Cros, C., Incardona, J.P., Scholz, N.L., Block, B.A., 2017. A novel cardiotoxic mechanism for a pervasive global pollutant. Sci. Rep. 7, 41476.
Campo, P., Venosa, A.D., Suidan, M.T., 2013. Biodegradability of Corexit 9500 and dispersed South Louisiana crude oil at 5 and 25 C. Environ. Sci. Technol. 47, 1960–1967.
Couillard, C.M., Lee, K., Légaré, B., King, T.L., 2005. Effect of dispersant on the composition of the water-accommodated fraction of crude oil and its toxicity to larval marine fish. Environ. Toxicol. Chem. 24, 1496–1504.
Dasgupta, S., Huang, I.J., McElroy, A.E., 2015. Hypoxia enhances the toxicity of corexit EC9500A and chemically dispersed southern louisiana sweet crude oil (MC-242) to sheepshead minnow (Cyprinodon variegatus) larvae. PLoS One 10, e0128939.
DeLorenzo, M., Key, P., Chung, K., Pisarski, E., Shaddrix, B., Wirth, E., Pennington, P., Wade, J., Franco, M., Fulton, M., 2018. Comparative toxicity of two chemical dispersants and dispersed oil in estuarine organisms. Arch. Environ. Contam. Toxicol. 74, 414–430.
Duan, J., Yu, Y., Li, Y., Li, Y., Liu, H., Jing, L., Yang, M., Wang, J., Li, C., Sun, Z., 2016. Low-dose exposure of silica nanoparticles induces cardiac dysfunction via neutrophil-mediated inflammation and cardiac contraction in zebrafish embryos. Nanotoxicology 10, 575–585.
Echols, B., Langdon, C., Stubblefield, W., Rand, G., Gardinali, P., 2018. A comparative assessment of the aquatic toxicity of Corexit 9500 to marine organisms. Arch.

Environ. Contam. Toxicol. 1–11.
Edmunds, R.C., Gill, J., Baldwin, D.H., Linbo, T.L., French, B.L., Brown, T.L., Esbaugh, A.J., Mager, E.M., Stieglitz, J., Hoenig, R., 2015. Corresponding morphological and molecular indicators of crude oil toxicity to the developing hearts of mahi mahi. Sci. Rep. 5, 17326.
Esbaugh, A.J., Mager, E.M., Stieglitz, J.D., Hoenig, R., Brown, T.L., French, B.L., Linbo, T.L., Lay, C., Forth, H., Scholz, N.L., 2016. The effects of weathering and chemical dispersion on Deepwater Horizon crude oil toxicity to mahi-mahi (Coryphaena hippurus) early life stages. Sci. Total Environ. 543, 644–651.
Esbaugh, A.J., Khursigara, A., Johansen, J., 2018. Toxicity in Aquatic Environments: The Cocktail Effect, Development and Environment. Springer, pp. 203–234.
Finn, R.D., Bateman, A., Clements, J., Coggill, P., Eberhardt, R.Y., Eddy, S.R., Heger, A., Hetherington, K., Holm, L., Mistry, J., 2013. Pfam: the protein families database. Nucleic Acids Res. 42, D222–D230.
Fuller, C., Bonner, J., Page, C., Ernest, A., McDonald, T., McDonald, S., 2004. Comparative toxicity of oil, dispersant, and oil plus dispersant to several marine species. Environ. Toxicol. Chem. 23, 2941–2949.
Garcia, T.I., Shen, Y., Crawford, D., Oleksiak, M.F., Whitehead, A., Walter, R.B., 2012. RNA-Seq reveals complex genetic response to deepwater horizon oil release in Fundulus grandis. BMC Genomics 13, 474.
Gray, J.L., Kanagy, L.K., Furlong, E.T., Kanagy, C.J., McCoy, J.W., Mason, A., Lauenstein, G., 2014. Presence of the Corexit component dioctyl sodium sulfosuccinate in Gulf of Mexico waters after the 2010 Deepwater Horizon oil spill. Chemosphere 95, 124–130.
Haas, B.J., Papanicolaou, A., Yassour, M., Grabherr, M., Blood, P.D., Bowden, J., Couger, M.B., Eccles, D., Li, B., Lieber, M., 2013. De novo transcript sequence reconstruction from RNA-seq using the Trinity platform for reference generation and analysis. Nat. Protoc. 8, 1494.
Haeseleer, F., Jang, G.-F., Imanishi, Y., Driessen, C.A., Matsumura, M., Nelson, P., Palczewski, K.S., 2002. Dual-substrate specificity short-chain retinol dehydrogenases from the vertebrate retina. J. Biol. Chem. 277, 45537–45546.
Hemmer, M.J., Barron, M.G., Greene, R.M., 2011. Comparative toxicity of eight oil dispersants, Louisiana sweet crude oil (LSC), and chemically dispersed LSC to two aquatic test species. Environ. Toxicol. Chem. 30, 2244–2252.
Incardona, J.P., 2017. Molecular mechanisms of crude oil developmental toxicity in fish. Arch. Environ. Contam. Toxicol. 73, 19–32.
Incardona, J.P., Collier, T.K., Scholz, N.L., 2004. Defects in cardiac function precede morphological abnormalities in fish embryos exposed to polycyclic aromatic hydrocarbons. Toxicol. Appl. Pharmacol. 196, 191–205.
Incardona, J.P., Swarts, T.L., Edmunds, R.C., Linbo, T.L., Aquilina-Beck, A., Sloan, C.A., Gardner, L.D., Block, B.A., Scholz, N.L., 2013. Exxon Valdez to Deepwater Horizon: comparable toxicity of both crude oils to fish early life stages. Aquat. Toxicol. 142, 303–316.
Incardona, J.P., Gardner, L.D., Linbo, T.L., Brown, T.L., Esbaugh, A.J., Mager, E.M., Stieglitz, J.D., French, B.L., Labenia, J.S., Laetz, C.A., 2014. Deepwater Horizon crude oil impacts the developing hearts of large predatory pelagic fish. Proc. Natl. Acad. Sci., 201320950.
Ivančič, I., Degobbis, D., 1984. An optimal manual procedure for ammonia analysis in natural waters by the indophenol blue method. Water Res. 18, 1143–1147.
Johansen, J.L., Allan, B.J., Rummer, J.L., Esbaugh, A.J., 2017. Oil exposure disrupts early life-history stages of coral reef fishes via behavioural impairments. Nat. Ecol. Evol. 1, 1146.
Jones, E.R., Martyniuk, C.J., Morris, J.M., Krasnec, M.O., Griffitt, R.J., 2017. Exposure to Deepwater Horizon oil and Corexit 9500 at low concentrations induces transcriptional changes and alters immune transcriptional pathways in sheepshead minnows. Comp. Biochem. Physiol. Part D Genomics Proteomics 23, 8–16.
Khursigara, A.J., Perrichon, P., Bautista, N.M., Burggren, W.W., Esbaugh, A.J., 2017. Cardiac function and survival are affected by crude oil in larval red drum, Sciaenops ocellatus. Sci. Total Environ. 579, 797–804.
Kloeblen, S., Stieglitz, J.D., Suarez, J.A., Grosell, M., Benetti, D.D., 2018. Characterizing egg quality and larval performance from captive mahi-mahi Coryphaena hippurus (Linnaeus, 1758) spawns over time. Aquac. Res. 49, 282–293.
Knollmann, B.C., Chopra, N., Hlaing, T., Akin, B., Yang, T., Ettensohn, K., Knollmann, B.E., Horton, K.D., Weissman, N.J., Holinstat, I., 2006. Casq2 deletion causes sarcoplasmic reticulum volume increase, premature Ca 2+ release, and catecholaminergic polymorphic ventricular tachycardia. J. Clin. Invest. 116, 2510–2520.
Kujawinski, E.B., Kido Soule, M.C., Valentine, D.L., Boysen, A.K., Longnecker, K., Redmond, M.C., 2011. Fate of dispersants associated with the Deepwater Horizon oil spill. Environ. Sci. Technol. 45, 1298–1306.
Langmead, B., Salzberg, S.L., 2012. Fast gapped-read alignment with Bowtie 2. Nat. Methods 9, 357–359.
Lanham, K.A., Plavicki, J., Peterson, R.E., Heideman, W., 2014. Cardiac myocyte-specific AHR activation phenocopies TCDD-induced toxicity in zebrafish. Toxicol. Sci. 141, 141–154.
Lee, R.H., Lolley, R.N., 1993. Purification and Characterization of Phosducin from Bovine Retina, Methods in Neurosciences. Elsevier, pp. 196–204.
Li, B., Dewey, C.N., 2011. RSEM: accurate transcript quantification from RNA-Seq data with or without a reference genome. BMC Bioinformatics 12, 323.
Li, M.X., Hwang, P.M., 2015. Structure and function of cardiac troponin C (TNNC1): implications for heart failure, cardiomyopathies, and troponin modulating drugs. Gene 571, 153–166.
Love, M.I., Huber, W., Anders, S., 2014. Moderated estimation of fold change and dispersion for RNA-seq data with DESeq2. Genome Biol. 15, 550.
Mager, E.M., Esbaugh, A.J., Stieglitz, J.D., Hoenig, R., Bodinier, C., Incardona, J.P., Scholz, N.L., Benetti, D.D., Grosell, M., 2014. Acute embryonic or juvenile exposure to Deepwater Horizon crude oil impairs the swimming performance of mahi-mahi (Coryphaena hippurus). Environ. Sci. Technol. 48, 7053–7061.
Magnuson, J.T., Khursigara, A.J., Allmon, E.B., Esbaugh, A.J., Roberts, A.P., 2018. Effects of Deepwater Horizon crude oil on ocular development in two estuarine fish species, red drum (Sciaenops ocellatus) and sheepshead minnow (Cyprinodon variegatus). Ecotoxicol. Environ. Saf. 166, 186–191.
McGruer, V., Pasparakis, C., Grosell, M., Stieglitz, J.D., Benetti, D.D., Greer, J.B., Schlenk, D., 2019. Deepwater Horizon crude oil exposure alters cholesterol biosynthesis with implications for developmental cardiotoxicity in larval mahi-mahi (Coryphaena hippurus). Comp. Biochem. Physiol. Part C Toxicol. Pharmacol. 220, 31–35.
Mu, J., Jin, F., Ma, X., Lin, Z., Wang, J., 2014. Comparative effects of biological and chemical dispersants on the bioavailability and toxicity of crude oil to early life stages of marine medaka (Oryzias melastigma). Environ. Toxicol. Chem. 33, 2576–2583.
National Academies of Sciences, E., Medicine, 2019. The Use of Dispersants in Marine Oil Spill Response. The National Academies Press, Washington, DC.
Pashmforoush, M., Pomiès, P., Peterson, K.L., Kubalak, S., Ross Jr, J., Hefti, A., Aebi, U., Beckerle, M.C., Chien, K.R., 2001. Adult mice deficient in actinin–associated LIM-domain protein reveal a developmental pathway for right ventricular cardiomyopathy. Nat. Med. 7, 591.
Pasparakis, C., Mager, E.M., Stieglitz, J.D., Benetti, D., Grosell, M., 2016. Effects of Deepwater Horizon crude oil exposure, temperature and developmental stage on oxygen consumption of embryonic and larval mahi-mahi (Coryphaena hippurus). Aquat. Toxicol. 181, 113–123.
Perrichon, P., Mager, E.M., Pasparakis, C., Stieglitz, J.D., Benetti, D.D., Grosell, M., Burggren, W.W., 2018. Combined effects of elevated temperature and Deepwater Horizon oil exposure on the cardiac performance of larval mahi-mahi, Coryphaena hippurus. PLoS One 13, e0203949.
Pilcher, W., Miles, S., Tang, S., Mayer, G., Whitehead, A., 2014. Genomic and genotoxic responses to controlled weathered-oil exposures confirm and extend field studies on impacts of the Deepwater Horizon oil spill on native killifish. PLoS One 9, e106351.
Ramachandran, S.D., Hodson, P.V., Khan, C.W., Lee, K., 2004. Oil dispersant increases PAH uptake by fish exposed to crude oil. Ecotoxicol. Environ. Saf. 59, 300–308.
Rooker, J.R., Kitchens, L.L., Dance, M.A., Wells, R.D., Falterman, B., Cornic, M., 2013. Spatial, temporal, and habitat-related variation in abundance of pelagic fishes in the Gulf of Mexico: potential implications of the Deepwater Horizon oil spill. PLoS One 8, e76080.
Schneider, C.A., Rasband, W.S., Eliceiri, K.W., 2012. NIH Image to ImageJ: 25 years of image analysis. Nat. Methods 9, 671.
Sehnert, A.J., Huq, A., Weinstein, B.M., Walker, C., Fishman, M., Stainier, D.Y., 2002. Cardiac troponin T is essential in sarcomere assembly and cardiac contractility. Nat. Genet. 31, 106.
Sørhus, E., Incardona, J.P., Furmanek, T., Goetz, G.W., Scholz, N.L., Meier, S., Edvardsen, R.B., Jentoft, S., 2017. Novel adverse outcome pathways revealed by chemical genetics in a developing marine fish. elife 6, e20707.
Steffy, D.A., Nichols, A.C., Kiplagat, G., 2011. Investigating the effectiveness of the surfactant dioctyl sodium sulfosuccinate to disperse oil in a changing marine environment. Ocean. Sci. J. 46, 299–305.
Stieglitz, J.D., Hoenig, R.H., Kloeblen, S., Tudela, C.E., Grosell, M., Benetti, D.D., 2017. Capture, transport, prophylaxis, acclimation, and continuous spawning of Mahi-mahi (Coryphaena hippurus) in captivity. Aquaculture 479, 1–6.
Whitehead, A., Triant, D., Champlin, D., Nacci, D., 2010. Comparative transcriptomics implicates mechanisms of evolved pollution tolerance in a killifish population. Mol. Ecol. 19, 5186–5203.
Whitehead, A., Pilcher, W., Champlin, D., Nacci, D., 2011. Common mechanism underlies repeated evolution of extreme pollution tolerance. Proc. R. Soc. Lond., B, Biol. Sci. 279, 427–433.
Whitehead, A., Dubansky, B., Bodinier, C., Garcia, T.I., Miles, S., Pilley, C., Raghunathan, V., Roach, J.L., Walker, N., Walter, R.B., 2012. Genomic and physiological footprint of the Deepwater Horizon oil spill on resident marsh fishes. Proc. Natl. Acad. Sci. 109, 20298–20302.
Xu, E.G., Mager, E.M., Grosell, M., Pasparakis, C., Schlenker, L.S., Stieglitz, J.D., Benetti, D., Hazard, E.S., Courtney, S.M., Diamante, G., 2016. Time-and oil-dependent transcriptomic and physiological responses to Deepwater Horizon oil in mahi-mahi (Coryphaena hippurus) embryos and larvae. Environ. Sci. Technol. 50, 7842–7851.
Xu, E.G., Khursigara, A.J., Magnuson, J., Hazard, E.S., Hardiman, G., Esbaugh, A.J., Roberts, A.P., Schlenk, D., 2017. Larval red drum (Sciaenops ocellatus) sublethal exposure to weathered Deepwater Horizon crude oil: Developmental and transcriptomic consequences. Environ. Sci. Technol. 51, 10162–10172.
Xu, E.G., Magnuson, J.T., Diamante, G., Mager, E., Pasparakis, C., Grosell, M., Roberts, A.P., Schlenk, D., 2018. Changes in microRNA–mRNA Signatures Agree with Morphological, Physiological, and Behavioral Changes in Larval Mahi-Mahi Treated with Deepwater Horizon Oil. Environ. Sci. Technol. 52, 13501–13510.